JOURNAL OF APPLIED ELECTROCHEMISTRY **27** (1997) 579–583

Performance of catalytically activated anodes in the electrowinning of metals

S. KULANDAISAMY, J. PRABHAKAR RETHINARAJ, S. C. CHOCKALINGAM, S. VISVANATHAN, K. V. VENKATESWARAN, P. RAMACHANDRAN, V. NANDAKUMAR

Central Electrochemical Research Institute, Karaikudi-630 006, India

Received 17 August 1995; revised 22 November 1996

The performance of titanium anodes coated with oxides of Ir–Co or Ir–Ta has been compared using long term polarization techniques under simulated electrowinning conditions. Possible reasons for anode failure are explained from SEM and XRD. Potentiodynamic studies in 2 M H_2SO_4 indicate that approximately 450 mV reduction in anode potential can be achieved with Ti/(Ir–Co) as against lead. This anode is also suitable in chloride contaminated sulfate electrolyte. The anode potential measurements in different electrowinning electrolytes indicate that a potential saving up to 370–420 mV can be achieved. It is interesting to note that mixed electrolyte containing sulfate and chloride behaves similarly to pure chloride electrolyte with respect to anode potential.

1. Introduction

The energy consumed in the electrowinning of metals accounts for a substantial portion of the overall cost of the metal production. Some 50–60% of the energy is consumed in the anode reaction alone, so that the appropriate selection of the anode is a prerequisite.

The relatively low cost of ruthenium oxide and its success in the chlor-alkali industry suggest its application in sulfate electrolyte. Preliminary laboratory tests have been attempted in sulfate electrolyte for electrowinning of Cu, Zn, Ni, Co and Mn using dimensionally stable anodes (DSA^R), graphite based and ceramic based (RuO_2–TiO_2) anodes [1]. Investigations on the effect of chemical composition and surface morphology revealed that the active layer of ruthenium oxide is corroded over a wide range of pH [2]. Platinum-clad anodes with titanium, tantalum and niobium have been tested and it has been found that loss of platinum is too high for commercial application, particularly in the case of electrolytes with sulfur containing organic additives. The complexing properties of noble metals with organic additives are the reason for such corrosion [3–5].

Iridium oxide alone, or in combination with other less expensive oxides has attracted attention as a possible anode coating for oxygen evolution. Thus, attempts have been made to test the IrO_2 coated anode in laboratory copper winning cells [6]. To make it cost effective, it is heavily doped or mixed with oxides of nonnoble metals like Ti, Zr, Ta, Sn, Mn, Co [7–14].

It is also known that oxides of iridium and cobalt having excess oxygen (p-type semiconductors) [15], are considered to be good for oxygen evolution [16]. Hence, it is likely that the 'mixed-crystal' oxides represent a crystalochemical system of their own inheriting their best properties [10, 17, 18] so as to exhibit maximum stability and catalytic activity.

Techniques of discerning and characterization of electrocatalytically coated titanium anodes have already been dealt with [19–21]. Critical evaluation of deactivation mechanisms of oxygen evolving anodes has been carried out, mainly employing galvanostatic methods and potential cycling at high current densities with emphasis on application in high speed electrogalvanization [22].

In this paper, the performances of Ti/(Ir–Co), Ti/(Ir–Ta), Activated lead electrode as anodes are compared with conventional electrodes under electrowinning conditions.

2. Experimental details

2.1. *Preparation of test electrodes*

For polarization experiments two main categories of anodes viz. catalytically activated titanium electrode (CATE) and activated lead electrode (ALE) were employed. Of the former type, two systems viz. Ti/(Ir–Co) and Ti/(Ir–Ta) were prepared by mechanically polishing titanium specimens with emery paper of 0/0–4/0 grade, successively, moistened with alcohol and subsequently degreased. The respective chloride salts in isopropyl alcohol which form the chelate consisting of 70 at % Ir and 30 at % Co or Ta (with Ir 3 g m^{-2}), was brush coated over the polished titanium strips of 2 cm × 16 cm, dried at about 80 °C and baked at 500 °C for 10 min in air. The process of painting, drying and baking was repeated until all the chelate had been consumed. Electrodes thus prepared were finally annealed at 500 °C for an hour. This optimum composition was arrived at by a comb-

ination of experimentation and literature information [8, 17, 23].

In the case of ALE, the titanium sponge particles were treated with $IrCl_3$ dissolved in isopropyl alcohol, thermally decomposed at 400 °C in a current of air to form a IrO_2 coating; subsequently the prepared activated sponge particles were anchored to the lead substrate by pressing at 250 kg cm^{-2}, the load of electrocatalyst being 10 g(Ir) m^{-2}. The working area of each electrode was 2 cm × 8 cm × 2 sides.

2.2. *Polarization studies*

Long term polarization experiments were carried out at an anode current density of 200 A m^{-2} in 0.5 M H_2SO_4 using a H-type glass cell with provision for continuous flow of electrolyte. The cyclic voltammetric (CV) studies were carried out using a Wenking potentioscan (model POS 73) coupled with a Rikadenki *X-Y-t* recorder. The area of the working electrode was 1 cm^2. For measurements of anode potential under electrowinning conditions in different electrolytes, an H-type glass cell was employed using the appropriate electrolyte at ambient temperature (30 °C). A Hg/Hg_2SO_4/0.5 M H_2SO_4 or a saturated calomel electrode (SCE) was used as the reference electrode, as the case may be, and a Pt wire gauze formed the counter electrode.

2.3. *Electrowinning of nickel*

For electrowinning experiments, a Ti/(Ir–Co) anode and a stainless steel cathode of size 16 cm × 2 cm were used (the immersion area being 8 cm × 2 cm). A two compartment PVC cell with a capacity of 1300 ml (cathode chamber 700 ml and anode compartment 600 ml) was used. Provision for continuous feeding of the fresh electrolyte into the cathode compartment and withdrawal of depleted electrolyte from the anode compartment was made. The anode and cathode compartments were separated by a 'Mytex' diaphragm of 35% porosity. The catholyte level was always maintained higher than that of the anolyte by about 1.5–2.0 cm in order to avoid back diffusion of the anolyte. The operating conditions are presented in Table 1.

Table 1. Electrowinning of nickel: operating conditions

Anode size (coating area)	8 cm × 2 cm
Electrolyte composition:	
Ni^{2+} concentration	60–70 g dm^{-3}
Boric acid	15–20 g dm^{-3}
Sodium sulfate	20 g dm^{-3}
Feed solution	pH 4
Current density	200 A m^{-2}
Feed rate	0.180 dm^3 h^{-1}
Temperature	30 °C
Catholyte	pH 2.5–3.5
Interelectrode distance	4.5 cm
Diaphragm material	Mytex
Acid concentration in anolyte	50 g dm^{-3}

3. Results and discussion

3.1. *Comparison of anode materials: electrochemical investigations*

3.1.1. Ti/(Ir–Co) and Ti/(Ir–Ta) systems: long term polarization studies. From Fig. 1 it is seen that both Ti/(70 at % Ir–30 at % Co) and Ti/(70 at % Ir–30 at % Ta) anodes possess a useful life of around one year with a steady anode potential. However, the anode potential for Ti/(Ir–Co) is lower than that for Ti/(Ir–Ta) to the extent of 100 mV, which is due to the higher resistivity of the oxides of Ta. Hence the Ti/(Ir–Co) anode system was taken for further study.

3.1.2. Ti/(Ir–Co) and lead: potentiodynamic studies. Figure 2 represents the potentiodynamic curves of a Ti/(Ir–Co) anode and a conventional lead anode in the potential range up to oxygen evolution in 200 g dm^{-3} H_2SO_4. The oxygen evolution potential of the former anode is 370 mV lower than that of the latter. This is in conformity with the potential measurements carried out under electrowinning conditions (cf. Table 2).

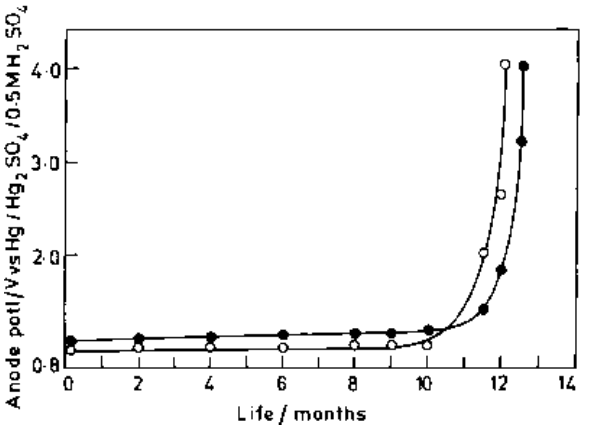

Fig. 1. Long term polarization curves: life against anode potential. Ir load: 3 g m^{-2}; current density: 200 A m^{-2}; temperature: 30 °C; electrolyte: 0.5 M H_2SO_4. Curves: (●) Ti/Ir–Ta and (○) Ti/Ir–Co.

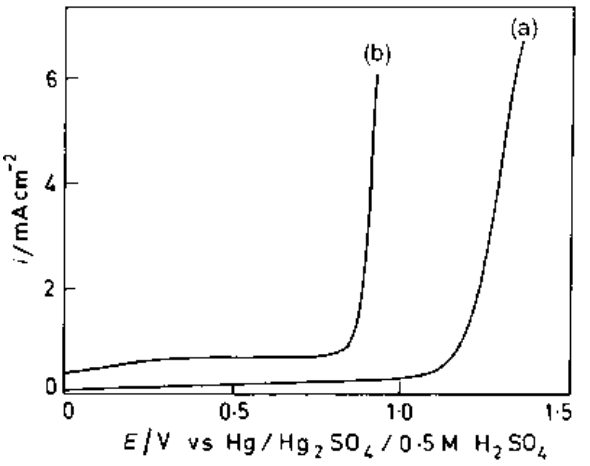

Fig. 2. Comparison of different anodes by potentiodynamic studies. Electrolyte: 200 g dm^{-3} H_2SO_4; scan rate: 10 mV s^{-1}. (a) Pb anode and (b) Ti/(Ir–Co) anode.

Table 2. Comparison of anode potential in different electrowinning processes /V vs NHE*

Anode	*Zinc*		*Nickel*			*Manganese*		*Copper*
	SO_4^{2-}	Cl^-	SO_4^{2-}	Cl^-	*Mixed*	SO_4^{2-}	Cl^-	SO_4^{2-}
Lead	2.06	–	2.10	–	–	2.19	–	2.09
Graphite	2.04	1.44	1.96	1.45	–	1.82	1.42	1.97
Ti/(Ir–Co) (70 at % Ir)	1.69	1.42	1.69	1.42	1.44	1.77	1.49	1.69

Operating conditions	*Zinc*	*Nickel*	*Manganese*	*Copper*
Concentration/M	Zn^{2+} 1.0 acid 1.0	Ni^{2+} 1.0 acid 0.5	Mn^{2+} 0.36 NH_4^+ 0.9–2 acid 0.5	Cu^{2+} 1.0 acid 1.7
Current density /A m^{-2}	400	200	450	250
Duration/min	15	15	15	15

3.1.3. Ti/(Ir–Co), lead and graphite: potential measurements in different electrolytes. Table 2 shows data collected with Ti/(Ir–Co) and conventional (lead /graphite) anodes for electrowinning of Zn, Ni, Cu and Mn. A voltage advantage of 370–420 mV can be achieved by using a Ti/(Ir–Co) anode with respect to the conventional lead anode in pure sulfate electrolytes, whereas in the case of chloride electrolyte, the voltage advantage over the graphite anode is marginal.

In the case of manganese electrolytes, a slight increase in anode potential is observed due to blocking of catalytic sites by the deposition of manganese dioxide. This occurs more in the case of sulfate electrolyte, than chloride.

3.2. *Influence of chloride addition to sulfate electrolyte on Ti/(Ir–Co) anode: CV studies*

In Fig. 3 curve (a) represents the CV of the anode in 200 g dm^{-3} H_2SO_4 and (b) that of the same in the mixed electrolyte containing 200 g dm^{-3} H_2SO_4 and 25 g dm^{-3} HCl. The addition of 25 g dm^{-3} HCl to H_2SO_4 reduces the potential by 200 mV. As a result, this anode is a candidate in chloride contaminated sulfate electrolyte from galvanizing industry wastes. In this context, the conventional anodes, lead and graphite, are suitable only in sulfate and chloride electrolyte, respectively, but are not suitable in mixed electrolyte.

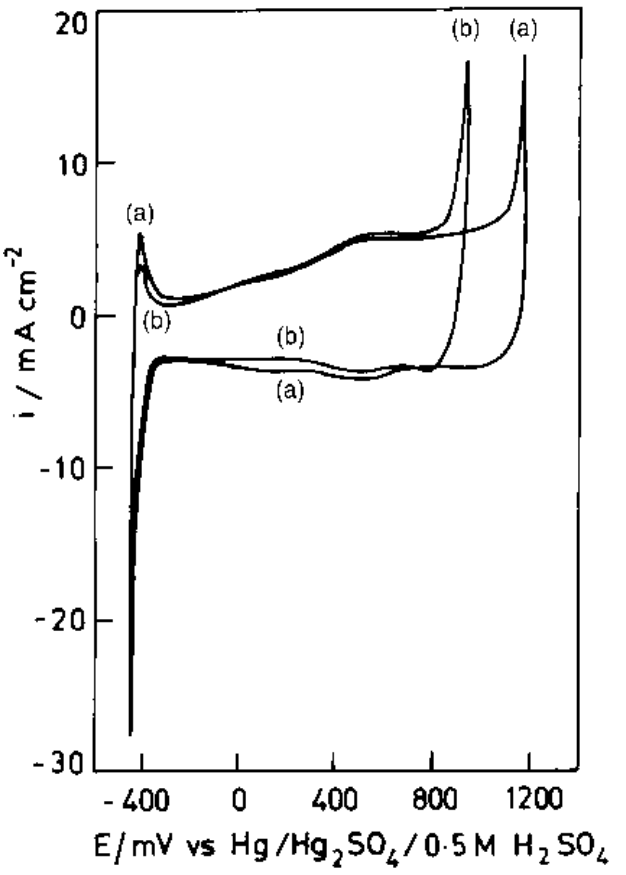

Fig. 3. Cyclic voltammogram illustrating the influence of different electrolytes on Ti/(Ir–Co) anode. Scan rate: 50 mV s^{-1}. Curves: (a) 200 g dm^{-3} H_2SO_4; (b) 200 g dm^{-3} H_2SO_4 + 25 g dm^{-3} HCl.

3.3. *Evaluation of Ti/(Ir–Co) and ALE anodes: electrowinning nickel*

Table 3 illustrates the influence of the anode/cathode current density on anode potential and cathode current efficiency. Saving in anode potential increases with current density, whereas the cathodic current efficiency falls at and above 300 A m^{-2}. The anode potential saving at the optimum current density of 200 A m^{-2} is 370–550 mV. The rise in anode potential with increase in current density for Ti/(Ir–Co) is not felt to the extent as that observed for the lead anode. This may be related to the fact that the Tafel slope (0.05 V) for oxygen evolution on IrO_2 is lower than that (0.12–0.15 V) of PbO_2 [24]. A similar trend is also likely in the (Ir–Co) system. On the lead anode, the presence of a thick oxide layer contributes to the higher resistivity, leading to an enhanced anode potential, whereas in the case of Ti/(Ir–Co), the larger surface area of the electrocatalyst with increased activity facilitates lowering of the effective current density, resulting in reduced anode potential.

Table 3. Influence of anode/cathode current density on the anode performance and cathode current efficiency in electrowinning nickel

Anode/cathode current density /A m^{-2}	*Anode potential* / V			*Saving in anode potential* / mV		*Cathode current efficiency* / %
	Pb	*Ti/Ir–Co*	*ALE*	*Ti/Ir–Co*	*ALE*	
50	1.90	1.70	–	200	–	85
100	2.00	1.72	–	280	–	90
200	2.10	1.73	1.55	370	550	95
300	2.20	1.75	1.57	450	630	86
400	2.28	1.77	1.58	510	700	80
500	2.35	1.79	1.59	560	760	80

Table 4 presents typical data collected in continuous electrolysis experiments with a nickel sheet as cathode and lead or Ti/(Ir–Co) as anode for longer duration runs. As already mentioned, a potential saving of about 400 mV was achieved in the case of the Ti/(Ir–Co) anode. This accounts for an energy saving of approximately 20%.

3.4. *Ti/(Ir–Co) anode: SEM and XRD studies*

Scanning electron micrographs of a Ti/(Ir–Co) oxide coated anode before and after one year of useful life are shown in Fig. 4. Fig. 4(a) represents the topography of the catalyst coated anode before employment in the long term polarization test. It reveals a more compact structure, with minimum micropores and cracks. Fig. 4(b) and (c) show the topography of the anode (with different magnifications) after one year of useful life. It is evident that the nature of the surface is partially modified due to the formation of cracks, macropores and exfoliation.

The failure of the anode is due to reactions occurring: (i) at the interface between the electrocatalyst and the electrolyte; (ii) through the pores and cracks in the coating; and (iii) at the interface between the titanium substrate and the electrocatalyst.

Based on the proposed mechanism of wear of RuO_2 [25], the most probable reactions in the case of IrO_2 occurring at the interface between the electrocatalyst and the electrolyte are:

$$IrO_2 + H_2O \longrightarrow IrO_3 + 2H^+ + 2e^-$$

$$IrO_3 \longrightarrow IrO_2 + O_{ads}$$

$$2O_{ads} \longrightarrow O_2$$

Another model proposed for dissolution of IrO_2 formed from Ir is shown in Fig. 5. The total amount of oxygen species remains constant, while the formation of oxide species grows at the expense of hydroxide species. Starting from $Ir(OH)_3$, a deprotonation step leads to the formation of $IrO(OH)_2$ with Ir in the tetravalent state. The first deprotonation step is connected with the colouration of the oxide film. After two additional deprotonation steps, IrO_3 is formed, with Ir in the hexavalent state, where oxygen is split off. Simultaneous uptake of one water molecule leads back to tetravalent iridium as the starting position for the cycle. Alternatively, IrO_3 may corrode into the electrolyte as IrO_4^{2-} [26].

Table 4. Comparison of data of anode potentials in electrowinning nickel

Experimental details	*Lead anode*	*Ti/(Ir–Co)*	*anode*
Duration /h	30	60	120
Anode potential /V	2.10	1.70	1.70

Diaphragm: Mytex (35% porosity)
Current efficiency: 95%

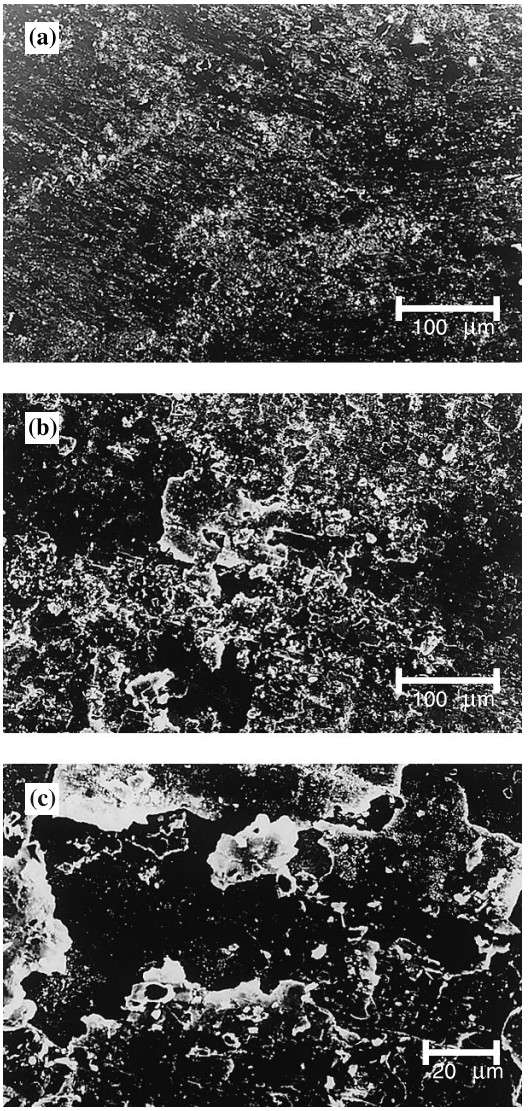

Fig. 4. SEM photographs of Ti/(Ir–Co) anode: (a) before use; (b) and (c) after use.

Figures 6(a) and (b) are the XRD patterns of the Ti/(Ir–Co) anodes before and after the long term polarization for one year. On comparison, the three characteristic peaks corresponding to the 'mixed-crystal oxides' of cobalt and iridium ($2\theta = 27.3°$, 35.7° and 39.8°) remain the same in both cases, except for the fact that only one peak ($2\theta = 35.7°$) is not predominant in the latter case. This may be due to anodic dissolution or structural change occurring during polarization. However, the general nature of

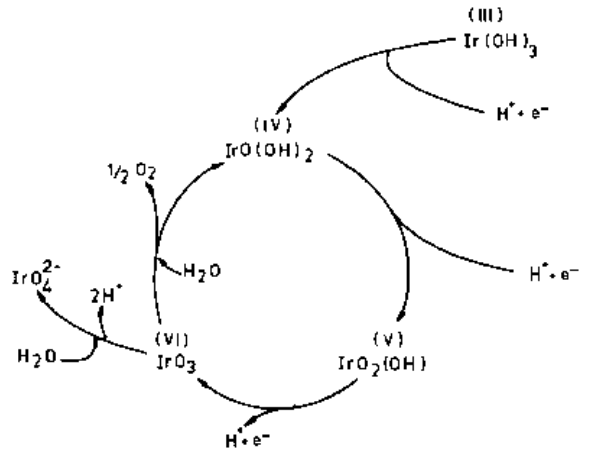

Fig. 5. Model for oxygen evolution and corrosion in IrO_2 electrodes [25].

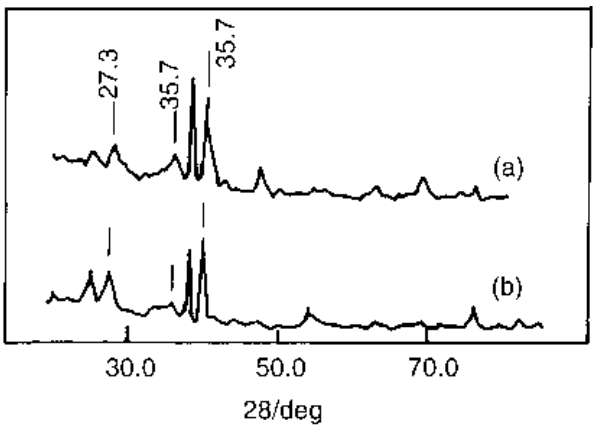

Fig. 6. XRD patterns of Ti/(Ir–Co) anode: (a) before use and (b) after use.

the XRD patterns of the two electrodes remains more or less the same.

The additional cracks and macropores developed during anodic polarization in the aggressive medium also facilitate the diffusion of oxygen and oxygenated species through the coating to reach the surface of the titanium substrate resulting in the formation of non-conducting TiO_2 film which results in only partial utilization of the electrocatalyst. Thus the catalytic anode fails at the end of its service life of one year, even though a sufficient quantity of electrocatalyst is still in the active state. The suggestion is supported by the fact that only 10–15% of the electrocatalyst is lost at the end of the service life of a Ti/(IrO_2–Ta_2O_5) anode [27]. This offers an opportunity for an in-depth study to re-utilize the once used anode.

4. Conclusions

(a) The failure of a catalytic anode is due to the combined effect of (i) anodic dissolution during oxygen evolution which occurs at the catalyst–electrolyte interface and (ii) the thick barrier film of TiO_2 grown at the titanium–electrocatalyst interface. The presence of such a barrier film is mainly responsible for partial utilization of the electrocatalyst.

(b) The anode potential for Ti/(Ir–Co) is lower than that of Ti/(Ir–Ta) to the extent of 100 mV under electrowinning conditions for a duration of one year.

(c) Electrical energy saving to the extent of 20% can be achieved.

(d) A major portion of the electrocatalyst remains unutilized which offers good scope for reactivation of the once used anode.

(e) The system investigated, [Ti/(Ir–Co)], may have scope in chloride contaminated sulfate electrolyte from secondary sources.

References

[1] Y. Liu, L. Wu and B. Yuan, *in* 'Energy Reduction Techniques in Metal Electrochemical Processes' (edited by R. G. Bautista and R. J. Wesely), Metallurgical Society, Pennsylvania, (1985), p. 331.
[2] G. Lodi, E. Sivieri, A. De. Battisti and S. Trasatti, *J. Appl. Electrochem.* **8** (1978) 135.
[3] A. J. Scarpellino Jr and J. L. Fischer, *J. Electrochem. Soc.* **129** (1982) 522.
[4] *Idem, ibid.* **129** (1982) 515.
[5] Ya. M. Kolotyrkin, V. V. Losev and A. N. Chemodanov, *Mater. Chem. Phys.* **19** (1988) 1.
[6] C. G. Ferron, 'Investigations of Precious Metal Coated Anodes in Copper Electrowinning', PhD. thesis, Columbia University, (1988).
[7] J. Rolewicz, Ch. Comninellis, E. Plattner and J. Hinden, *Electrochim. Acta* **33** (1988) 573.
[8] Ch. Comninellis and G. P. Vercesi, *J. Appl. Electrochem.* **21** (1991) 335.
[9] N. Balko and P. H. Nguyen, *ibid.* **21** (1991) 678.
[10] New Materials Developed in Japan, (edited by T. Gomi), Toray Research Centre, Inc. (1986), p. 162.
[11] Yu. E. Roginskaya, O. V. Morozova, E. N. Loubnin, A. V. Papov, Yu. I. Ulitina, V. V. Zhurov, S. A. Ivanov and S. Trasatti, *J. Electrochem. Soc. Faraday Trans.* **89** (1993) 1707.
[12] R. Mraz and J. Krysa, *J. Appl. Electrochem.* **24** (1994) 1262.
[13] Y. Kamegaya, K. Sasaki, M. Oguri, T. Asaki, H. Kobayashi and T. Mitamura, *Electrochim. Acta* **40** (1995) 889.
[14] F. Noguchi, S. Matsumura, T. Iida, T. Mitamura, Y. Kamegaya and Y. Arai, *Denki Kagaku Oyobi Kogyo Butsuri Kagaku* **52** (1984) 276.
[15] S. Trasatti, *Electrochim. Acta* **36** (1991) 225.
[16] S. R. Morrison, 'The Chemical Physics of Surfaces', Plenum Press, New York (1978), p. 331.
[17] S. Kulandaisamy, J. Prabhakar Rethinaraj, S. C. Chockalingam and S. Visvanathan, *Mater. Chem. Phys.* **35** (1993) 176.
[18] Ya. M. Kolotyrkin, V. V. Losev, D. M. Shub and Yu. E. Roginskaya, *Sov. Electrochem.* **15** (1979) 245.
[19] T. Loucka, *J. Appl. Electrochem.* **7** (1977) 211.
[20] F. Hine, M. Yasuda, T. Noda, T. Yoshida and J. Okada, *J. Electrochem. Soc.* **126** (1979) 1437.
[21] J. Prabhakar Rethinaraj, S. Kulandaisamy, S. C. Chockalingam, S. Visvanathan and K. S. Rajagopalan, Proc. Symp. Adv. Electrochemicals, CECRI, Karaikudi, Apr. (1984), p. 2.1.
[22] G. N. Martelli, R. Ornelas and G. Faita, *Electrochim. Acta* **39** (1994) 1551.
[23] S. C. Chockalingam, J. Prabhakar Rethinaraj, S. Kulandaisamy and S. Visvanathan, *Bull. Electrochem.* **6** (1990) 198.
[24] P. Ramachandran, K. V. Venkateswaran, V. Nandakumar, S. Kulandaisamy, J. Prabhakar Rethinaraj, S. C. Chockalingam and S. Visvanathan, *ibid.* **8** (1992) 291.
[25] G. Barral, J. Guitton, C. Montella and F. Vergara, *Surf. Technol.* **10** (1980) 25.
[26] R. Kotz, H. Neff and S. Stucki, *J. Electrochem. Soc.* **131** (1984) 72.
[27] Ch. Comninellis and E. Plattner, *Proc. Electrochem. Soc.* **89–10** (1989) 229.